Calculating landscape surface area from digital elevation models

Jeff S. Jenness

Abstract There are many reasons to want to know the true surface area of the landscape, especially in landscape analysis and studies of wildlife habitat. Surface area provides a better estimate of the land area available to an animal than planimetric area, and the ratio of this surface area to planimetric area provides a useful measure of topographic roughness of the landscape. This paper describes a straightforward method of calculating surface-area grids directly from digital elevation models (DEMs), by generating 8 3-dimensional triangles connecting each cell centerpoint with the centerpoints of the 8 surrounding cells, then calculating and summing the area of the portions of each triangle that lay within the cell boundary. This method tended to be slightly less accurate than using Triangulated Irregular Networks (TINs) to generate surface-area statistics, especially when trying to analyze areas enclosed by vector-based polygons (i.e., management units or study areas) when there were few cells within the polygon. Accuracy and precision increased rapidly with increasing cell counts, however, and the calculated surface-area value was consistently close to the TIN-based area value at cell counts above 250. Raster-based analyses offer several advantages that are difficult or impossible to achieve with TINs, including neighborhood analysis, faster processing speed, and more consistent output. Useful derivative products such as surface-ratio grids are simple to calculate from surface-area grids. Finally, raster-formatted digital elevation data are widely and often freely available, whereas TINs must generally be generated by the user.

Key words elevation, landscape, surface area, surface ratio, terrain ruggedness, TIN, topographic roughness, rugosity, triangulated irregular network

Landscape area is almost always presented in terms of planimetric area, as if a square kilometer in a mountainous area represents the same amount of land area as a square kilometer in the plains. Predictions of home ranges for wildlife species generally use planimetric area even when describing mountain goats (*Oreamnos americanus*) and pumas (*Felis concolor*). But if a species' behavior and population dynamics are functions of available resources, and if those resources are spatially limited, I suggest assessing resources using surface area of the landscape.

Surface area also is a basis for a useful measure of landscape topographic roughness. The surface-area ratio of any particular region on the landscape can be calculated by dividing the surface area of that region by the planimetric area. For example, Bowden et al. (2003) found that ratio estimators of Mexican spotted owl (*Strix occidentalis lucida*) population size were more precise using a version of this surface-area ratio than with planimetric area.

Many wildlife species are identified with topographic attributes, including the topographic roughness or ruggedness of the landscape. For example, Wakelyn (1987) found greater numbers of Rocky Mountain bighorn sheep (*Ovis canadensis canadensis*) in mountain ranges with higher measures of topographic relief, and Gionfriddo and Krausman (1986) found that desert bighorn sheep (*O. c. mexicana*) generally were found at or near

Author's address: United States Department of Agriculture Forest Service, Rocky Mountain Research Station, 2500 S. Pine Knoll Drive, Flagstaff, AZ 86001, USA; e-mail: jeffj@jennessent.com.

the tops of steep slopes and close to steep, rocky escape terrain. Warrick and Cypher (1998) found that kit foxes (*Vulpes macrotis mutica*) near Bakersfield, California were strongly associated with low topographic ruggedness, and Wiggers and Beasom (1986) found that Texas white-tailed deer (*Odocoileus virginianus texanus*) appeared to prefer areas with less topographic ruggedness than desert mule deer (*O. hermionus crooki*).

A variety of methods exist in the literature for measuring terrain irregularity. Hobson (1972) described some early computational methods for estimating surface area and discussed the concept of surface-area ratios. Beasom (1983) described a method for estimating land surface ruggedness based on the intersections of sample points and contour lines on a contour map, and Jenness (2000) described a similar method based on measuring the density of contour lines in an area. Mandelbrot (1983:29, 112–115) described the concept of a "fractal dimension" in which the dimension of an irregular surface lies between 2 (representing a flat plain) and 3 (representing a surface that goes through every point within a volume). Calculating this fractal dimension can be very challenging computationally, and Polidori et al. (1991), Lam and De Cola (1993), and Lorimer et al. (1994) discussed a variety of methods for estimating the fractal dimension for a landscape. An estimate of surface area also could be derived from slope and aspect within a cell (Berry 2002), although Hodgson (1995) demonstrated how most slope-aspect algorithms generate values reflecting an area 1.6–2 times the size of the actual cell. Surface-area values derived with this method would therefore be unduly influenced by adjacent cells.

In this paper I demonstrate a straightforward method for calculating the surface area of landscapes from digital elevation models (DEMs), which are widely and freely available within the United States and are becoming increasingly available throughout the rest of the world (Jet Propulsion Laboratory 2003, Gesch et al. 2002, United States Geological Survey [USGS] 2002). I compared surface-area values produced by this method with values produced with triangulated irregular networks (TINs), which are 3-dimensional vector representations of a landscape created by connecting the DEM elevation values into a continuous surface. Unlike DEMs, these TINs are continuous vector surfaces and therefore can be precisely measured and clipped. I also discuss advantages and disadvantages of this method in comparison to using TINs.

Methods

Throughout this paper I refer to "grids," and in this case a grid is a specific type of geographic data used by ArcInfo and ArcView. A grid essentially is a raster image in which each pixel is referred to as a "cell" and has a particular value associated with it. For USGS DEMs, the cell value reflects the elevation in meters of the central point in that cell.

The method described here derives surface areas for a cell using elevation information from that cell plus the 8 adjacent cells. For example, given a sample elevation grid, this method would calculate the surface area for the cell with elevation value "165" based on the elevation values of that cell plus the 8 surrounding cells (Figure 1). That central cell and its surrounding cells are pictured in 3-dimensional space as a set of adjacent columns, each rising as high as its specified elevation value (Figure 2*b*).

The 3-dimensional centerpoints of each of these 9 cells are used to calculate the Euclidian distance between the focal cell's centerpoint and the centerpoints of each of the 8 surrounding cells. I use the term "surface length" to highlight the 3-dimensional character of this line; this is not the planimetric (horizontal) distance between cell centerpoints. Next, calculate the surface lengths of the lines that connect each of the 8 surrounding cells with the ones adjacent to it to get the lengths of the sides of the 8 triangles projected in 3-dimensional space that all meet at the centerpoint of the central cell (Figure 3*b*).

These surface lengths are calculated using the Pythagorean theorem. Thus, for any 2 cell center-

210	190	170	155	140	135
204	183	165	145	125	120
200	175	160	122	110	100
208	187	165	150	126	120

Figure 1. Small Digital Elevation Model (DEM) with elevation values overlaid on each cell. Use a "moving window" approach to calculate the surface area for each cell based on the elevation from that cell plus the elevation values for the 8 surrounding cells.

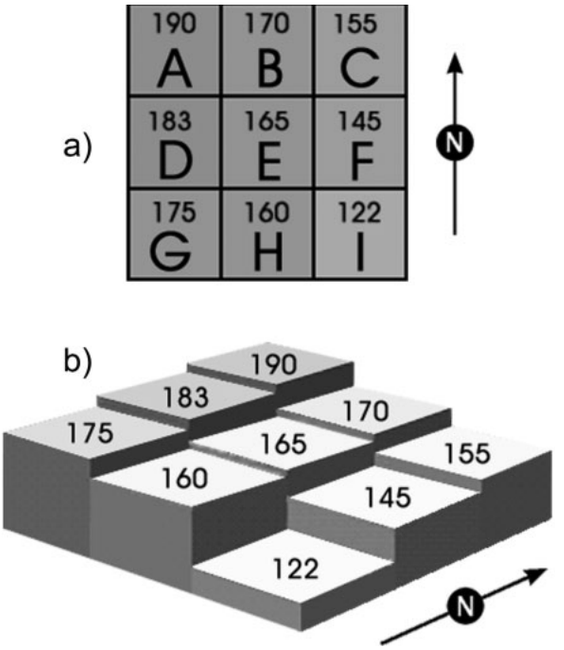

Figure 2. Using the elevation values from Figure 1, cells A-I represent cells necessary to calculate the surface area for the central cell (a). The cells can be visualized as a set of adjacent columns each rising to their respective elevation values (b).

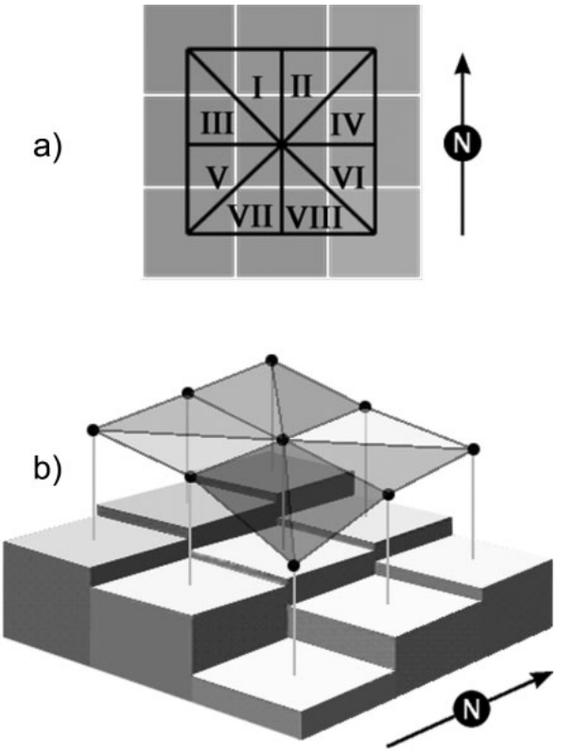

Figure 3. Calculate 3-dimensional lengths between the center of the central cell to the centers of the surrounding cells, and the lengths between adjacent surrounding cells, to get the edge lengths for the triangles I–VIII (a). These triangles form a continuous surface over the 9 cells (b).

points P and Q:

$$a^2 + b^2 = c^2 \qquad \text{or} \qquad c = \sqrt{a^2 + b^2},$$

where

a = planimetric (horizontal) distance from P to Q,
b = difference in elevation between P and Q,
c = surface distance from P to Q.

Distance "b" is easy to calculate because it is simply the absolute difference between the 2 cell elevation values. Distance "a" is even easier for the cells directly to the north, east, south, and west, because it is simply the length of the side of the cells (L). For cells in diagonal directions, use the Pythagorean theorem again to calculate that distance "a" = $\sqrt{2L^2}$.

Conducting these calculations for the central cell plus the 8 adjacent cells produces the lengths for the sides of the 8 triangles connecting the center of the central cell to the centers of the 8 adjacent cells. However, this leads to a minor complication because these triangles extend past the cell boundary and therefore represent an area larger than the cell. The triangles must be trimmed to the cell boundaries (Figure 4) by dividing all the length values by 2. This action is justified based on the Side-Angle-Side similarity criterion for similar triangles (Euclid 1956:204), which states that "If two triangles have one angle equal to one angle and the sides about the equal angles proportional, the triangles will be equiangular and will have those angles equal which the corresponding sides subtend." Each original triangle is "similar" to its corresponding clipped triangle because the 2 sides extending from the center cell in the original triangle are exactly twice as long as the respective sides in the clipped triangle, and the angles defined by these 2 sides are the same in each triangle. Therefore, the third side of the clipped triangle must be exactly half as long as the corresponding side of the original triangle.

Now when the lengths of the 3 sides are used to calculate the area of the triangle, the 3 sides will represent only the portion of the triangle that lies within the cell boundaries. For example, using the elevation DEM from Figure 1, and assuming that

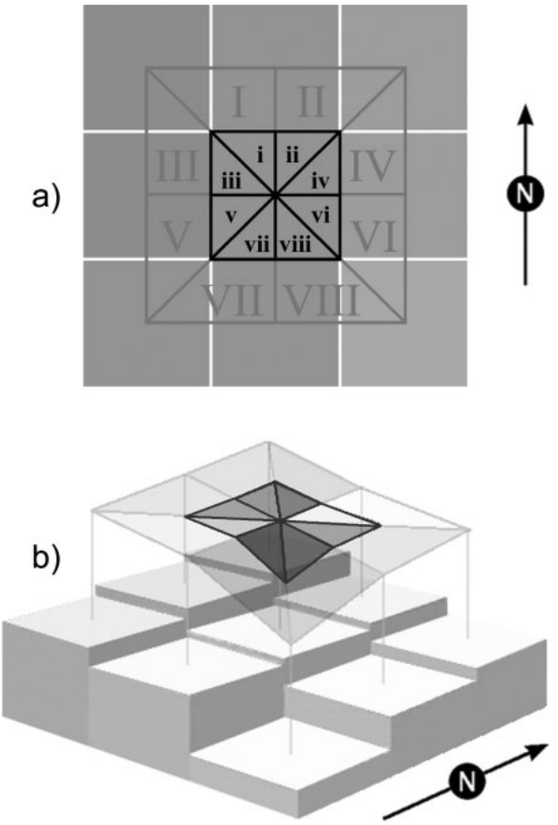

Figure 4. Surface area within the cell should only reflect the areas of triangles i–viii (a), so trim the triangles to the cell boundaries (b) by dividing all the triangle side lengths by 2.

cells are 100 m on a side and that elevation values are also in meters, begin by calculating the 16 triangle edge lengths for the 8 3-dimensional triangles radiating out from the central cell E (Figures 2*a*, 3*a*). Divide these surface lengths in half to get the sides for triangles i–viii in Figure 4 (Table 1), and use those lengths to determine the surface areas for each triangle (Table 2). The area of a triangle given the lengths of sides *a, b,* and *c* (Abramowitz and Stegun 1972) is calculated as:

$$\sqrt{s(s-a)(s-b)(s-c)},$$

where

$$s = \frac{a+b+c}{2}.$$

Finally, sum the 8 triangle area values to get final surface-area value for the cell (10,280.48 m^2 in this example). This is 280 m^2 more than planimetric area of the cell (100 m × 100 m = 10,000 m^2).

Table 1. Elevation values for the 9 cells in Figure 2*a* are used to generate 16 surface lengths for the edges of the 8 triangles in Figure 3*a*. These surface lengths are divided in half to get the edges for the 8 triangles in Figure 4*a*.

Triangle edge	Planimetric length (m)	Elevation difference (m)	Surface length (m)	Surface length / 2 (m)
$\overline{AB}$	100.00	20	101.98	50.99
$\overline{BC}$	100.00	15	101.12	50.56
$\overline{DE}$	100.00	18	101.61	50.80
$\overline{EF}$	100.00	20	101.98	50.99
$\overline{GH}$	100.00	15	101.12	50.56
$\overline{HI}$	100.00	38	106.98	53.49
$\overline{AD}$	100.00	7	100.24	50.12
$\overline{BE}$	100.00	5	100.12	50.06
$\overline{CF}$	100.00	10	100.50	50.25
$\overline{DG}$	100.00	8	100.32	50.16
$\overline{EH}$	100.00	5	100.12	50.06
$\overline{FI}$	100.00	23	102.61	51.31
$\overline{EA}$	141.42	25	143.61	71.81
$\overline{EC}$	141.42	10	141.77	70.89
$\overline{EG}$	141.42	10	141.77	70.89
$\overline{EI}$	141.42	43	147.81	73.91

Testing

I tested the accuracy of this method by generating a surface-area grid in which the cell value for each cell reflected the surface area within that cell. I then calculated total surface area within several sets of polygons randomly distributed across the landscape. I initially calculated polygonal surface areas using the methods described in this paper and then compared those with surface-area values calculated via TINs. As 3D vector representations of the landscape, these TINs provide a true continuous surface based on the DEM elevation values. They provide a good baseline to compare against

Table 2. Calculations of true surface area for triangles i–viii (Figure 4*a*) based on the 16 edge lengths from Table 1.

Triangle	Edges	Edge lengths (m)	Triangle area (m^2)
i	$\overline{EA}$, $\overline{AB}$, $\overline{BE}$	71.81, 50.99, 50.06	1,276.22
ii	$\overline{BE}$, $\overline{BC}$, $\overline{EC}$	50.06, 50.56, 70.89	1,265.48
iii	$\overline{AD}$, $\overline{DE}$, $\overline{EA}$	50.12, 50.80, 71.81	1,272.95
iv	$\overline{EC}$, $\overline{CF}$, $\overline{EF}$	70.89, 50.25, 50.99	1,280.88
v	$\overline{DE}$, $\overline{DG}$, $\overline{EG}$	50.80, 50.16, 70.89	1,273.94
vi	$\overline{EF}$, $\overline{FI}$, $\overline{EI}$	50.99, 51.31, 73.91	1,306.88
vii	$\overline{EG}$, $\overline{EH}$, $\overline{GH}$	70.89, 50.06, 50.56	1,265.48
viii	$\overline{EH}$, $\overline{EI}$, $\overline{HI}$	50.06, 73.91, 53.49	1,338.64

because they can be precisely clipped to polygon boundaries and measured.

I used elevation data derived from 15 1º × 1º USGS 1:250,000-scale DEMs downloaded from the USGS EROS data center website (USGS 2002). I converted these DEMs into ArcInfo grids and combined them into a single seamless grid using the ArcView Spatial Analyst extension (Environmental Systems Research Institute [ESRI] 2000*b*), and then projected the final grid into the UTM Zone 12 projection using the "Reproject Grids" extension (Quantitative Decisions 1999). The projected grid contained approximately 19 million cells. This data set was developed for use in a separate study (Ganey et al. 1999), and as part of that study I clipped the grid to an irregular-shaped polygon covering mountainous central portions of Arizona and western New Mexico (Figure 5). Because of the clip, only about 6.8 million of these cells contained elevation values. Cell dimensions were approximately 92 m × 92 m, and the entire region containing data covered 54,850 km^2.

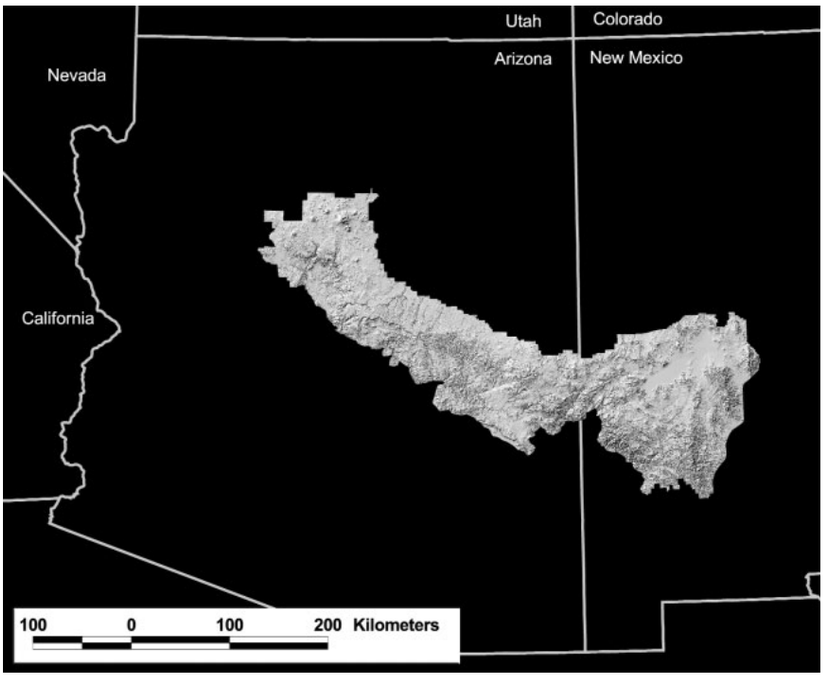

Figure 5. Sample elevation data derived from 1º × 1º USGS 1:250,000-scale DEMs, containing approximately 6.8 million elevation values arrayed across the mountainous central portions of Arizona and western New Mexico.

Generating polygons

Accuracy under ideal conditions. To generate an accuracy baseline, I used polygons that conformed perfectly to cell edges. These polygons had none of the edge-effect problems found in normal irregularly shaped polygons, and therefore surface-area calculations within them should give results as close as possible to values determined by TIN-based calculations. I generated 500 such rectangular polygons with random lengths, widths, and locations (Figure 6*a*) with the only provisos being that they lay completely within the digital elevation model and that their edges conform perfectly to the cell edges. These rectangles ranged in area from 16 ha (18 cells) to 33,661 ha (39,601 cells). I then classified them into 13 size classes based on cell counts to see if there were any changes in accuracy as cell counts increased.

Accuracy in real-world conditions. I used a real-world example of 983 irregularly shaped watersheds originally developed for a separate research effort (Ganey et al. 1999) (Figure 6*b*). These watersheds ranged in size from 1.7 ha (2 cells) up to 33,980 ha (39,579 cells). As with the rectangles, I classified these polygons into 13 size classes based on cell size.

Accuracy vs. area-to-edge ratio. Finally, to examine accuracy as a function of the relationship between area and edge length, I generated a set of 700 elliptical polygons of random shape and orientation, but all with an internal area equal to approximately 215 ha (250 cells) (Figure 6c). I chose this size because, based on visual examination of the data, it appeared to be at approximately the upper boundary of the size range at which most variation in accuracy seems to occur, and therefore ellipses of this size should be sensitive to edge-effect problems. Because of the random arrangement of these ellipses, actual cell counts ranged from 205–274 cells ($\bar{x}$ = 251, SD = 4). Hence, I standardized area-to-edge ratio

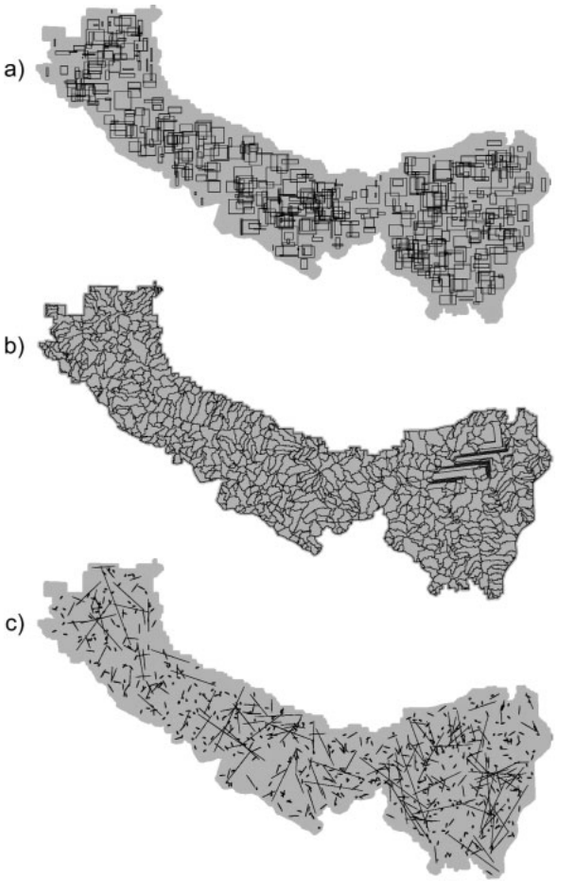

Figure 6. Three sets of sample polygons used to test the accuracy of this method: a) 500 rectangular polygons randomly distributed across the landscape, whose boundaries exactly correspond with cell edges in the DEM so that both grid-based and TIN-based calculations of surface areas from these polygons will reflect the exact same underlying surface; b) 983 watersheds distributed across the landscape, providing real-world examples of irregularly shaped polygons; and c) 700 elliptical polygons of random shape and orientation (some of which are so elongated that they appear as lines), each with a size approximately equal to 215 ha (250 cells), randomly distributed across the landscape.

values based on the area and circumference of a perfect circle (i.e., the shape with the maximum possible area-to-edge ratio) with an area equivalent to 250 cells. Each ellipse received an area-to-edge value of:

$$\frac{\left(\dfrac{\text{Ellipse Area}}{\text{Perfect Circle Area}}\right)}{\left(\dfrac{\text{Ellipse Circumference}}{\text{Perfect Circle Circumference}}\right)}.$$

By this method, a perfect circle would receive an area-to-edge ratio of 1 while an infinitely long ellipse would receive a value of 0. I suspected that the accuracy would improve as the area-to-edge ratios approached 1, so I generated these 700 ellipses such that there would be 70 ellipses in each 0.1-unit range between 0 and 1 (i.e., 70 ellipses between 0 and 0.1, 70 between 0.1 and 0.2, etc.). This allowed me to assess accuracy over the full range of possible area-to-edge values.

Generating surface areas per polygon

I used the ArcView 3.2a GIS package with Spatial Analyst 2.0 (ESRI 2000*a, b*), plus the Surface Areas and Ratios from Elevation Grid extension (Jenness 2001*a*), to automate the surface-area calculations and to provide surface area statistics for the various sets of test polygons.

To calculate TINs for each polygon, I used ArcView with 3D Analyst (ESRI 1998) along with the Surface Tools for Points, Lines and Polygons extension (Jenness 2001*b*) to generate the polygon statistics. When generating a TIN from a grid data set, ArcView automatically selects the grid cell centerpoints to use with the TIN based on a vertical accuracy that you specify (ESRI 1997:32). A vertical accuracy of "10," for example, would produce a TIN surface model that was always within 10 vertical map units of the grid cell centers. ArcView does not accept a vertical accuracy of "0," so I generated TINs with vertical accuracies of 0.0001 m.

Statistical tests

I evaluated how close the grid-based surface-area values for each polygon came to the TIN-based values by generating a ratio of the TIN-based value to the grid-based value. By this method, a value of 1 indicates a perfect match. For each sample polygon data set, I generated boxplots of these ratios within each size class to examine the range of values among size classes. I then calculated correlation between the grid-based and TIN-based values using Spearman's rank correlation (r_s) because my surface-area values were not normally distributed. Finally, I checked for any potential multiplicative or additive biases by computing simple linear regression analyses, forced through the origin, for each data set and checking that the slope values were approximately equal to 1. I used SPSS 9.0 (SPSS, Inc. 1998) for all statistical analyses.

Results

The ratios of TIN-based to grid-based surface-area values for the 500 rectangles tended to be very close to 1 in all size classes (Figure 7), with slightly more variation at the lower size classes. The TIN-based values tended to be slightly but consistently higher than the grid-based values at cell counts >2,500, with mean ratio values ranging from 1.000007–1.000018. Regression through the origin produced a slope value of 1.000 (SE < 0.0001, 95% CI = 1.000–1.000). The TIN-based surface areas and the grid-based surface areas were highly correlated (r_s > 0.999). The ratios among the 983 watersheds also tended to come close to 1 in all size classes (Figure 8). Again, the greatest variability was at the smallest size class (cell count < 250). TIN-based calculations again were highly correlated with grid-based calculations (r_s > 0.999). Regression through the origin produced a slope value of 1.000 (SE < 0.0001, 95% CI = 1.000–1.000).

The set of 700 standardized ellipses showed a general trend toward increasing accuracy and precision as the area-to-edge ratios approached 1, with the range of values in each class becoming progressively narrower (Figure 9). The median value was close to 1 in all cases, but the correlation between TIN-based and grid-based calculations among these smaller polygons was lower than with the larger polygons (r_s = 0.825). Regression through the origin produced a slope value of 0.999 (SE = 0.001, 95% CI = 0.998–1.001).

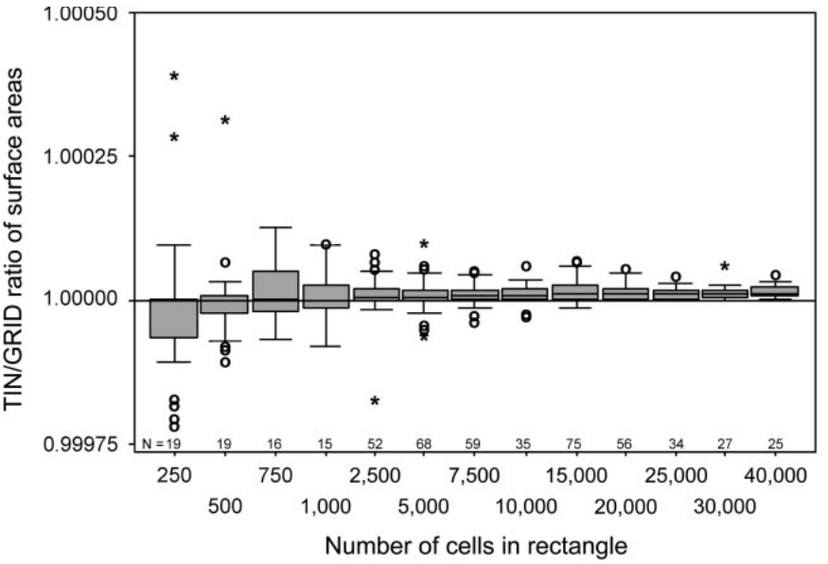

Figure 7. Boxplots representing the ratio of TIN-based surface area over grid-based surface area, for the 500 randomly distributed rectangles from Figure 6*a*. The edges of these rectangles perfectly correspond with the edges of the underlying grid cells. Horizontal bars within boxes represent the median, the tops and bottoms of the boxes represent the 75th and 25th quantiles, and the whiskers represent the range excluding outliers and extremes. Outliers (values >1.5 box lengths from box) are displayed with the symbol "o" and extremes (values >3 box lengths from the box) are displayed with the symbol "*".

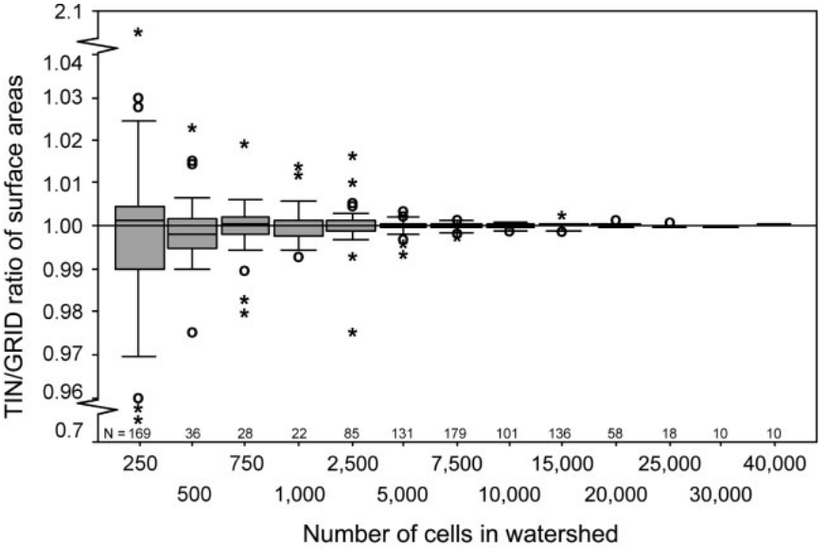

Figure 8. Boxplots representing the ratio of TIN-based surface area over grid-based surface area, for the 983 watersheds from Figure 6*b*.

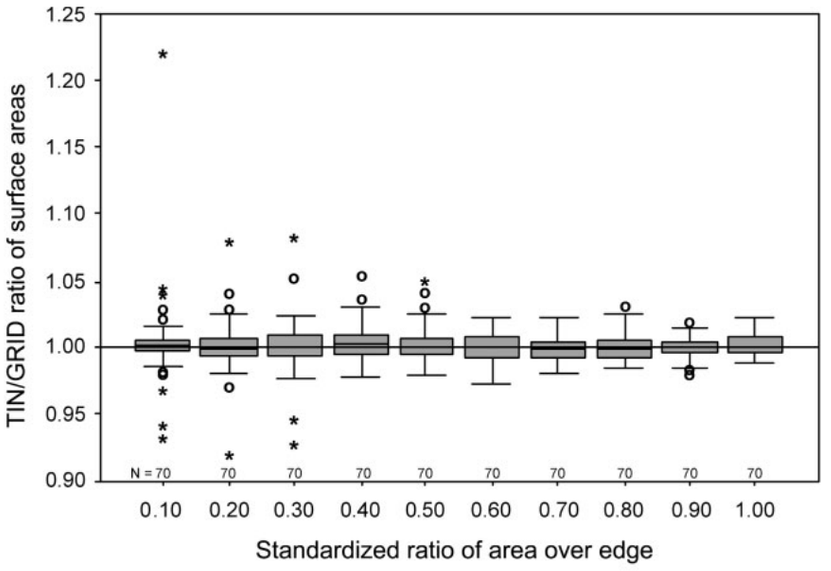

Figure 9. Boxplots representing the ratio of TIN-based surface area over grid-based surface area, for the 700 standardized ellipses from Figure 6c. These ellipses have a constant internal area but random shapes, orientations, and locations. They are classified according to their standardized area-to-edge ratio, where 0 reflects an infinitely stretched ellipse and 1 reflects a perfect circle.

Discussion

Raster data sets such as DEMs and surface-area grids are inherently less accurate and precise than vector data sets such as TINs and polygons. The most accurate measure of the surface area within a polygon should include all the area within the polygon and no more. Except in unusual circumstances, raster data sets do not meet this criterion because cells in a raster data set do not sit perfectly within polygon boundaries. Cells typically overlap the polygon edges, and GIS packages generally consider cells to be "inside" a polygon only if the cell center lies inside that polygon. Therefore, raster representations of polygons have a stair-stepped appearance, incorporating some areas outside the polygon and missing some areas inside. Cells lying directly on the border always lie partly inside and partly outside a polygon, but they are always classified as being entirely inside or outside the polygon. Therefore, the accuracy of a surface-area measurement within a polygon is affected by what proportion of the cells lie along the polygon edge. This proportion typically decreases as the number of cells increases, so accuracy should also increase as the number of cells increases.

Although cell-based calculations are inherently less precise and accurate than vector-based calculations, this method still came extremely close to duplicating results from TIN-based surface-area calculations. Accuracy and precision increased as the number of cells increased. Under ideal conditions in which the test polygon edges corresponded exactly to the cell edges, this method produced nearly identical surface-area calculations. The regression slope values and extremely low standard error values demonstrated that there was no apparent bias in this method. Surface-area values computed using this method did tend to be slightly lower than those computed with TIN-based methods, but only on the order of about 0.1–0.2 m^2/ha, suggesting that this method did well at duplicating TIN-based values for grid cells that do not lie on polygon boundaries.

Under conditions more analogous to real-world situations, this method produced variable accuracies when there were <250 cells in a particular polygon and good-to-excellent accuracy at cell counts >250. At higher cell counts, the grid-based values were almost identical to TIN-based values.

The analysis of the 983 watersheds showed considerably more variability when the polygons contained <250 grid cells (Figure 8), which is reasonable considering the inherent imprecision in grid-based processes. Polygons containing relatively few grid cells would be most affected by errors caused by grid cells lying on the polygon boundary. The proportion of interior cells to edge cells increased as overall cell counts increased, causing more of the total polygon surface area to be derived from the highly accurate interior cell values. This trend was also illustrated in the calculations involving the 700 standardized ellipses, in which variability steadily decreased as area-to-edge ratios approached 1. The range of values in the 0.0–0.1 class was 4 times as large as the range in the 0.5–0.6 class and 7 times the range in the 0.9–1.0 class

(Figure 9). The ellipses with area-to-edge ratios closer to 1 had proportionally fewer edge cells, and therefore more of the surface-area calculations were based on accurate interior cell values.

Advantages and disadvantages of this method over using TINs

Given that the testing and comparisons presented in this paper assume that TIN-based calculations are the most accurate, it is natural to wonder why we should not just use TINs. TINs offer many advantages over raster data sets for many aspects of surface analysis. As vector objects, they are not affected by the edge-effect problems that are unavoidable with raster-based methods and are considerably more reliable and accurate over areas with relatively low cell counts (Wang and Lo 1999). They generally take up much less space on the hard drive than raster data, and they are often more aesthetically pleasing to display (Mahdi et al. 1998). However, the methods described in this paper offer advantages that are difficult or impossible to achieve with TINs.

Surface-area ratio grids. Surface-area grids may easily be standardized into surface-area ratio grids by dividing the surface-area value for each cell by the planimetric area within that cell. These surface-area ratio grids are useful as a measure of topographic roughness or ruggedness over an area and conceivably could be used as friction or cost grids for analysis of movement (such grids would steer the predicted direction of movement based on the topographic roughness of a cell). Because these ratio grids are in raster format, they also lend themselves to neighborhood-based statistics as described below.

Neighborhood analysis. In many cases we are not interested in values of individual cells but rather the values in a region around those cells. This is especially common when we are interested in phenomena over multiple spatial scales. For example, neighborhood analysis can be applied to surface-area grids to produce grids representing the sum, maximum, minimum, mean, or standard deviation of surface areas within neighborhoods of increasing size surrounding each cell. These neighborhoods can take on a variety of shapes, including squares, doughnuts, wedges, and irregular shapes (ESRI 1996:103). Neighborhood analysis is simple with raster data but very difficult with TINs.

Faster processing speed. Given comparable resolutions, TINs take longer to generate and work with than raster data sets. A process that takes minutes or seconds with a raster data set may take several hours with a TIN.

More consistent and comparable output. TINs often are generated according to a specified accuracy tolerance in which the surface must come within a specific vertical distance of each elevation point, meaning that a TIN surface rarely goes exactly through all the base elevation points on the landscape. This also means that 2 TINs may have been generated with different tolerances, and therefore surface statistics derived from those TINs may not be comparable. This is especially problematic when the TINs are derived using whatever default accuracy is suggested by the software, which generally varies from analysis to analysis based on the range of elevation values in the DEM. The method described in this paper, however, will always produce a surface-area grid that takes full advantage of all the elevation points in the DEM. Surface-area statistics derived from any region may then be justifiably compared with any other region.

Data is readily available. Digital elevation models, at least within the United States, are widely available and often freely downloadable off the Internet (Gesch et al. 2002, USGS 2002). Worldwide data from the 2000 Shuttle Radar Topography Mission is steadily becoming available (Jet Propulsion Laboratory 2003). TINs, however, are rarely available (the author has never seen them available on the Internet) and therefore must be generated by the user.

More accurate proportions of available resources. By weighting resource maps with underlying surface-area values, land managers and researchers can generate more accurate extents and proportions of resources within a particular region. This is especially true if any of the resources are especially associated with particularly steep or flat areas.

The method described in this paper provides a straightforward and accurate way to generate surface-area values directly from a DEM. People who use this method will face accuracy and precision errors when they calculate surface areas within vector-based polygons simply because of problems inherent in extracting data from raster-based sources (like grids and DEMs) and applying them to precisely defined vector objects (like management units and study areas). However, accuracy and precision problems diminish rapidly as cell counts increase and become negligible for most purposes

at cell counts >250. The calculations involved, while most effectively computed in a GIS package, also could easily be done in a spreadsheet. For users of ESRI's ArcView 3.x software with Spatial Analyst, the author offers a free extension that automates the process and directly produces surface-area and surface-ratio grids from grid-formatted DEMs. This extension may be downloaded from the author's website at http://www.jennessent.com/arcview/surface_areas.htm or from the ESRI ArcScripts site at http://arcscripts.esri.com/details.asp?dbid=11697.

Acknowledgments. I thank J. Aguilar-Manjarrez, L. I. Engelman, J. L. Ganey, L. M. Johnson, R. King, D. Whitaker, G. White, and an anonymous reviewer for their valuable assistance with reviewing early drafts of this manuscript.

Literature cited

ABRAMOWITZ, M., AND I. A. STEGUN. 1972. Handbook of mathematical functions with formulas, graphs and mathematical tables. Dover Publications, New York, New York, USA.

BEASOM, S. L. 1983. A technique for assessing land surface ruggedness. Journal of Wildlife Management 47: 1163–1166.

BERRY, J. K. 2002. Use surface area for realistic calculations. Geoworld 15(9): 20–21.

BOWDEN, D. C., G. C. WHITE, A. B. FRANKLIN, AND J. L. GANEY. 2003. Estimating population size with correlated sampling unit estimates. Journal of Wildlife Management 67: 1–10.

ENVIRONMENTAL SYSTEMS RESEARCH INSTITUTE. 1996. Using the ArcView spatial analyst: advanced spatial analysis using raster and vector data. Environmental Systems Research Institute, Redlands, California, USA.

ENVIRONMENTAL SYSTEMS RESEARCH INSTITUTE. 1997. Using ArcView 3D analyst: 3D surface creation, visualization, and analysis. Environmental Systems Research Institute, Redlands, California, USA.

ENVIRONMENTAL SYSTEMS RESEARCH INSTITUTE. 1998. ArcView 3D analyst. (ArcView 3.x Extension). Version 1. Environmental Systems Research Institute, Redlands, California, USA.

ENVIRONMENTAL SYSTEMS RESEARCH INSTITUTE. 2000*a*. ArcView GIS 3.2a. Environmental Systems Research Institute, Redlands, California, USA.

ENVIRONMENTAL SYSTEMS RESEARCH INSTITUTE. 2000*b*. ArcView spatial analyst. (ArcView 3.x Extension). Version 2. Environmental Systems Research Institute, Redlands, California, USA.

EUCLID. 1956. The thirteen books of Euclid's elements: translated with introduction and commentary by Sir Thomas L. Heath. Volume 2 (Books III–IX). Second Edition Unabridged. Dover Publications, New York, New York, USA.

GANEY, J. L., G. C. WHITE, A. B. FRANKLIN, AND J. P. WARD, JR. 1999. Monitoring population trends of Mexican spotted owls in Arizona and New Mexico: a pilot study. Study plan RM-4251–6–1. Rocky Mountain Research Station, Flagstaff, Arizona, USA.

GESCH, D., M. OIMOEN, S. GREENLEE, C. NELSON, M. STEUCK, AND D. TYLER. 2002. The national elevation dataset. Photogrammetric Engineering & Remote Sensing 68: 5–11.

GIONFRIDDO, J. P., AND P. R. KRAUSMAN. 1986. Summer habitat use by mountain sheep. Journal of Wildlife Management 50: 331–336.

HOBSON, R. D. 1972. Chapter 8 - surface roughness in topography: quantitative approach. Pages 221–245 *in* R. J. Chorley, editor. Spatial analysis in geomorphology. Harper & Row, New York, New York, USA.

HODGSON, M. E. 1995. What cell size does the computed slope/aspect angle represent? Photogrammetric Engineering & Remote Sensing 61: 513–517.

JENNESS, J. 2000. The effects of fire on Mexican spotted owls in Arizona and New Mexico. Thesis, Northern Arizona University, Flagstaff, USA.

JENNESS, J. 2001*a*. Surface areas and ratios from elevation grid. (ArcView 3.x Extension). Jenness Enterprises. Available online at http://www.jennessent.com/arcview/surface_areas.htm (accessed October 2003).

JENNESS, J. 2001*b*. Surface tools for points, lines and polygons. (ArcView 3.x Extension). Version 1.3. Jenness Enterprises. Available online at http://www.jennessent.com/arcview/surface_tools.htm [date accessed October 2003].

JET PROPULSION LABORATORY. 2003. Shuttle Radar Topography Mission (Web Page). Available online at http://www.jpl.nasa.gov/srtm/ (accessed October 2003).

LAM, N. S. N., AND L. DECOLA. 1993. Fractals in geography. PTR Prentice-Hall, Englewood Cliffs, New Jersey, USA.

LORIMER, N. D., R. G. HAIGHT, AND R. A. LEARY. 1994. The fractal forest: fractal geometry and applications in forest science. United States Department of Agriculture Forest Service, North Central Forest Experiment Station, General Technical Report; NC-170. St. Paul, Minnesota, USA.

MAHDI, A., C. WYNNE, E. COOPER, L. ROY, AND K. SHAW. 1998. Representation of 3-D elevation in terrain databases using hierarchical triangulated irregular networks: a comparative analysis. International Journal of Geographical Information Science 12: 853–887.

MANDELBROT, B. B. 1983. The fractal geometry of nature. W. H. Freeman, New York, New York, USA.

POLIDORI, L., J. CHOROWICZ, AND R. GUILLANDE. 1991. Description of terrain as a fractal surface, and application to digital elevation model quality assessment. Photogrammetric Engineering & Remote Sensing 57: 1329–1332.

QUANTITATIVE DECISIONS. 1999. Reproject Grids (ArcView 3.x extension): Quantitative Decisions. Available online at http://arcscripts.esri.com/details.asp?dbid=11368 (accessed October 2003).

SPSS, INC. 1998. SPSS 9.0 for Windows. SPSS, Chicago, Illinois, USA.

UNITED STATES GEOLOGICAL SURVEY. 2002. 1:250,000-scale digital elevation models. (Web Page). Available online at: ftp://edcftp.cr.usgs.gov/pub/data/DEM/250/. [date accessed October 2003].

WAKELYN, L. A. 1987. Changing habitat conditions on bighorn sheep ranges in Colorado. Journal of Wildlife Management 51: 904–912.

WANG, K., AND C-P. LO. 1999. An assessment of the accuracy of triangulated irregular networks (TINs) and lattices in ARC/INFO. Transactions in GIS 3: 161–174.

WARRICK, G. D., AND B. L. CYPHER. 1998. Factors affecting the spa-

tial distribution of San Joaquin kit foxes. Journal of Wildlife Management 62:707–717.

WIGGERS, E. P., AND S. L. BEASOM. 1986. Characterization of sympatric or adjacent habitats of 2 deer species in West Texas. Journal of Wildlife Management 50:129–134.

Jeff Jenness is a wildlife biologist with the United States Forest Service's Rocky Mountain Research Station in Flagstaff, Arizona. He received his B.S. and M.S. in forestry, as well as an M.A. in educational psychology, from Northern Arizona University. Since 1990 his research has focused primarily on issues related to Mexican spotted owls in the southwestern United States. He has also become increasingly involved in GIS-based analyses, and in 2000 he started a GIS consulting business in which he specializes in developing GIS-based analytical tools. He has worked with universities, businesses, and governmental agencies around the world, including a long-term contract with the Food and Agriculture Organization of the United Nations (FAO), for which he relocated to Rome, Italy for 3 months. His free ArcView tools have been downloaded from his website and the ESRI ArcScripts site over 100,000 times.

Associate editor: *White*